Effect of adsorbed concentration on the radiative rate enhancement of photoexcited molecules embedded in single microspheres

P. Sandeep and Prem Ballabh Bisht

Citation: The Journal of Chemical Physics **123**, 204713 (2005); doi: 10.1063/1.2126665
View online: http://dx.doi.org/10.1063/1.2126665
View Table of Contents: http://scitation.aip.org/content/aip/journal/jcp/123/20?ver=pdfcov
Published by the AIP Publishing

Effect of adsorbed concentration on the radiative rate enhancement of photoexcited molecules embedded in single microspheres

P. Sandeep and Prem Ballabh Bisht[a)]
Department of Physics, Indian Institute of Technology Madras, Chennai 600 036, India

(Received 8 June 2005; accepted 27 September 2005; published online 23 November 2005)

The variation of the molecular density in a single microcavity and its influence on the radiative rate enhancement (RRE) are reported here. The quality factors of the observed morphology-dependent resonances (MDRs) of the microcavity remain unchanged in the absence of any absorbing effects. In contrast, the MDRs tend to disappear in the presence of strong absorption even due to the self-absorption by the molecule. Time-resolved fluorescence studies reveal the fact that the value of RRE decreases with an increase in the adsorbed concentration of the molecules. The results have been explained in terms of a detuning parameter, which is a function of the refractive index of the microcavity. The increased dispersing capability of the microsphere upon increasing its molecular density has been found to be responsible for the observed decrease in RRE. © *2005 American Institute of Physics*. [DOI: 10.1063/1.2126665]

I. INTRODUCTION

Micrometer-sized dielectric particles of symmetric shape have been studied in recent years as excellent tools to explain the light-matter interactions.[1] Especially, the case of spherical microcavity has attracted a large attention due to its inherent simplicity.[2–4] The total internal reflection of light inside the cavity at its interface with the surrounding medium allows the natural modes of oscillation of the cavity to occur at specific frequencies. These modes are known as morphology-dependent resonances (MDRs) as their properties depend on the size, shape, and refractive index of the microcavity. The amplifying and energy-storing capabilities of MDRs have been found to be useful in the applications such as low threshold lasing,[5,6] enhanced energy transfer,[7,8] and biosensing.[9]

The radiative rate enhancement (RRE) of an excited atom or a molecule is of great importance since the experimental control over the pathway for excited-state deactivation can be obtained. This problem has been dealt with theoretically by calculating the transition rates by varying the transition frequency and the physical properties of the microcavity.[10,11] A theoretical treatment of the spontaneous emission of a two-level atom coupled to the narrow cavity resonance was proposed in terms of the Hermitian modes of the universe by Lai *et al.*[12] The expression for the RRE in terms of the mode densities of photons with and without the cavity was put forward by Yokoyama and Bronson.[13] A modified expression by separating the density of states within the cavity into resonant and background contributions was given by Arnold.[14] The enhancement was found to contain both $1/r$ and $1/r^2$ components where r is the radius of the microcavity. A quantum-mechanical treatment for the spontaneous emission from a two-level atom inside a dielectric sphere[15] and the spontaneous decay of an excited two-level atom in the presence of dispersing and absorbing dielectric bodies have been also studied.[16]

The modification of the spontaneous emission decay rate from chelated europium ions in microdroplets has been reported by Lin *et al.*[17] RRE has also been observed in Rhodamine 6G (R6G) confined in levitated ethylene glycol microdroplets.[18,19] The cavity quantum electrodynamics (QED) effects were reported to be responsible for the reduction in the fluorescence lifetime for pyrene[20] and 9-amino acridine hydrochloride hydrate (9AAHH) doped in polymer microspheres.[21]

Recently it has been shown that the intracavity power is extremely sensitive to the variation of the effective refractive index of the cavity mode near the resonance in an integrated optical microdisk.[22] It was also shown that quartz microspheres can be used to detect protein concentration by measuring the shift of the MDR as a function of the adsorbed concentration.[23] Based on the first-order perturbation theory, a theoretical explanation of the shift in the position of MDR for a small change in the refractive index of the outer medium or the radius of the microsphere has also been developed.[24] The formation of a nanolayer of adsorbed biological macromolecules on single microspheres has been characterized with the help of the shift of the MDR at two different wavelengths.[25] But, as yet, to the best of our knowledge, the effect of adsorbed concentration on both the steady-state and the time-resolved fluorescences of a molecule embedded in a microcavity has not been studied experimentally. Therefore in this paper, we present the observed changes in the RRE caused by the change in the molecular density inside a cavity. This has been explained on the basis of a change in the refractive index of the microcavity.

This paper is organized as follows. Section II gives the experimental details. The theoretical aspects of MDR and RRE are given in Sec. III. The results and discussion

[a)]Also at: Chemical Physics and Molecular Biology Group, IIT Madras, India. Electronic mail: bisht@iitm.ac.in

(Sec. IV) has been divided into four parts. Section IV A gives the experimentally observed MDR in the fluorescence spectra of dye-doped single microspheres. The theoretical fitting and the influence of absorption on the spectra and the quality factors of the MDR are also described here. Section IV B gives the effect of MDR on the radiative rate and the estimation of RRE from the experiments. In Sec. IV C, we introduce the detuning parameter, which is related to the refractive-index-based shift of a MDR. Section IV D gives a theoretical simulation of the detuning parameter that explains the experimental observations due to the change in the refractive index. The conclusions are given in Sec. V.

II. EXPERIMENT

The details of the experimental procedure for sample preparation and steady-state spectral measurements are given elsewhere.[21] Briefly, the microspheres of polymethyl methacrylate (PMMA) were immersed in solutions of varying concentrations of the dye 9AAHH (Aldrich) in spectrograde methanol for about 15 h. The microspheres were washed with distilled water and dried before transferring to a glass plate for measurements. The absorption measurements were done to estimate the concentration of the dye in microparticles. It was found to be ~100 times less than that of the doping solution. However, the concentrations mentioned here correspond to those of the doping solutions, unless otherwise specified. The steady-state fluorescence spectra of these dye-impregnated microspheres were measured with an epifluorescence microscope (Nikon Eclipse E-400) with the help of a monochromator and a photomultiplier tube (PMT). The excitation source was a superhigh-pressure Hg lamp equipped with a filter at 365 nm with a bandpass of 50 nm. For time-resolved measurements, a 40 ps pulsed laser at 408 nm (Pilas, Advanced Photonics) was used as an excitation source. The fluorescence from the single microsphere was directly fed to the PMT and the decay profiles were recorded by the time-correlated single-photon counting card (TC900, Edinburgh Instruments). The decay profiles were deconvoluted with the instrument response function (IRF) of the excitation pulse and were fitted with single and biexponential functions using standard software. The goodness of the fit was estimated by reduced χ^2 and weighted residuals. For a good fit, the value of χ^2 was around one and the residuals were distributed evenly on both sides of the fitted curve.

III. THEORETICAL CONSIDERATIONS

A. Morphology-dependent resonances (MDRs)

The fluorescence spectrum of the dye embedded in a single polymer microsphere shows ripple structures. These structures are built upon the background fluorescence of the dye. The observed structures are sensitive to the size and refractive index of the microsphere, and are known as MDR, which result from the Mie scattering phenomena. The positions of the MDR in the experimental spectra can be obtained theoretically as follows.

The ratio of the scattering cross section of the microsphere to its geometric cross section is known as the scattering efficiency and is given by

$$Q_{\mathrm{sca}} = \frac{2}{x^2}\sum_{n=1}^{\infty}(2n+1)(|a_n|^2+|b_n|^2), \tag{1}$$

where $x=2\pi r/\lambda$ is known as the size parameter. Here λ is the wavelength of the scattered light and r is the radius of the microsphere. The coefficients a_n and b_n are functions of the spherical Bessel $[j_n(x)]$ and Hankel $[h_n(x)]$ functions of the first kind and are given as

$$a_n = \frac{j_n(x)[mxj_n(mx)]' - m^2 j_n(mx)[xj_n(x)]'}{h_n^{(1)}(x)[mxj_n(mx)]' - m^2 j_n(mx)[xh_n^{(1)}(x)]'}, \tag{2a}$$

and

$$b_n = \frac{j_n(x)[mxj_n(mx)]' - j_n(mx)[xj_n(x)]'}{h_n^{(1)}(x)[mxj_n(mx)]' - j_n(mx)[xh_n^{(1)}(x)]'}. \tag{2b}$$

Here m represents the ratio of the refractive index of the cavity to that of the surrounding medium. The integer n denotes the order of the spherical Bessel and Hankel functions describing the radial field distribution and is known as the angular mode number. The number of maxima in the radial dependence of the mode is given by l which is termed as the mode order. The observed resonance peaks in a theoretically simulated Mie scattering efficiency curve of a microsphere are identified by their corresponding mode numbers (n) and mode orders (l).

B. Modification of radiative rate in a cavity

Upon photoexcitation, the coupling of the transition moment of the molecule with the MDR of the cavity increases the final density of states available for the emitting photon. This is responsible for the increase in the radiative rate of the molecule following Fermi's golden rule. This was first proposed by Purcell[26] for the case of a nuclear magnetic medium coupled to a resonant electrical circuit. The RRE in this case is given as

$$\xi = 3DQ\lambda^3/4\pi^2 V_m, \tag{3}$$

where D is the mode degeneracy, Q is the quality factor, and V_m is the mode volume. The modification in the radiative rate can be measured by the time-resolved fluorescence of the molecule by embedding it in a microcavity as well as in a bulk medium. It has been shown that RRE (ξ) can then be expressed as[13]

$$\xi = \frac{\int_0^\infty \rho_c(\nu)P(\nu)d\nu}{\int_0^\infty \rho_f(\nu)P(\nu)d\nu}. \tag{4}$$

Here the mode density of the photons in the presence of the cavity is denoted by $\rho_c(\nu)$, while that in the bulk is indicated by $\rho_f(\nu)$. $P(\nu)$ represents the transition rate per mode. Later, a theoretical expression of RRE was developed by Arnold[14] by separating the density of states within the microparticle into resonant and background contributions. The RRE of 9AAHH embedded in PMMA microspheres has been found to be in agreement with this.[21]

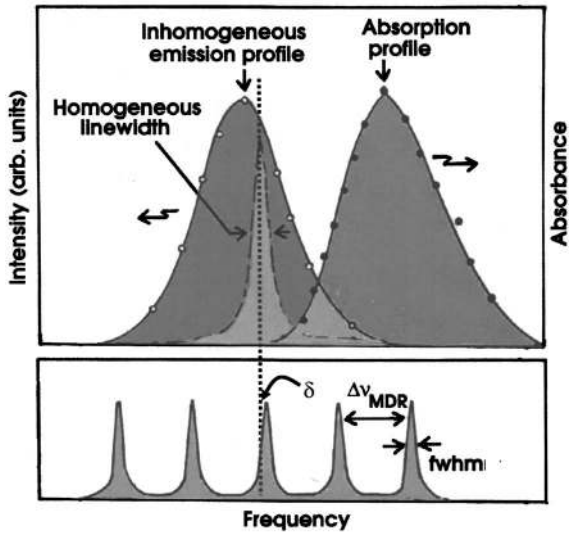

FIG. 1. Schematic diagram representing the various contributions for RRE: absorption profile (-●-) and fluorescence emission profile (-○-) of the molecule. The overlap between the fluorescence and absorption spectra contributes to the self-absorption effect. When a MDR of the microcavity (—) falls within the homogeneous linewidth of the molecule (---) the density of state is increased according to Eq. (4) that results in RRE.

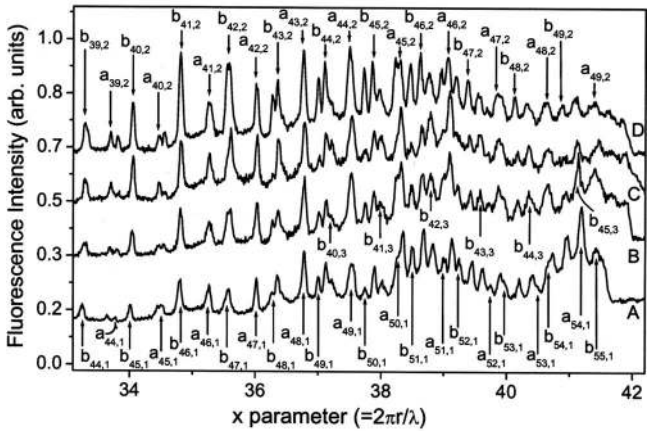

FIG. 2. Fluorescence spectra of 9AAHH in ~3-μm-radius single PMMA microsphere as a function of concentration. The concentrations are (A) 0.5 mM, (B) 5 mM, (C) 20 mM, and (D) 100 mM. The x parameter [Eq. (1)] is related to the radius of the particle and therefore it incorporates the variations arising out of the changes, if any, in the particle radius for the sake of a common plot (see text for details). All the curves are analyzed for the cavity modes of the first three orders. For clarity of presentation, the first-order TE ($b_{n,l}$) and TM ($a_{n,l}$) modes are tagged on the bottom curve (A), and the second-order modes are tagged on the top curve (D) while the third-order modes are tagged on curve (B).

Figure 1 shows a modified schematic diagram[3] of the various contributions influencing the interaction between the MDR and the radiative transition of a molecule. The reduction in the microsphere diameter increases the free spectral range of the MDR ($\Delta\nu_{\mathrm{MDR}}$). For a small size of the microsphere it is possible to have a condition that only a single MDR interacts within the homogeneous linewidth (Γ_h) of the emitter. In other words, when $\Delta\nu_{\mathrm{MDR}} > \Gamma_h > \gamma$ where γ represents the full width at half maximum (FWHM) of the interacting MDR,[17] the RRE can be approximated as

$$\xi \cong \Delta\nu_{\mathrm{MDR}}/\Gamma_h, \tag{5}$$

where $\Delta\nu_{\mathrm{MDR}} = (\arctan\sqrt{m^2-1})/(2\pi r\sqrt{m^2-1})$ and ξ (RRE) is the ratio of the measured radiative rate of the molecule in the presence of the cavity to that in a bulk medium.

IV. RESULTS AND DISCUSSIONS

A. Influence of self-absorption on the quality factors

Figure 2 shows the observed fluorescence spectra of 9AAHH embedded in single PMMA microspheres of ~3 μm radius by varying the dye concentration. The peak positions of the modes observed in the fluorescence spectra are simulated with the scattering efficiency [Eq. (1)]. The theoretical simulation for a portion of the spectrum (D) is shown in Fig. 3. The MDR are identified for their polarization [either transverse electric ($b_{n,l}$) or transverse magnetic ($a_{n,l}$)]. Their corresponding mode numbers and mode orders are also determined. It can be seen that the MDR peaks of the observed spectrum match well with those of the simulation for a microsphere of $r=2.807$ μm and $m=1.49$. As seen from the expression for $\Delta\nu_{\mathrm{MDR}}$ [*vide supra*, Eq. (5)] the position of the MDR in the spectra can shift either due to the change in (i) r (for fixed m), (ii) m (for fixed r), or (iii) both r and m. The spectra in Fig. 2 correspond to single microparticles of approximately the same radius as estimated visually from the scale of the microscope. The other spectra of Fig. 2 fit well with the simulations of $r=2.805\pm0.004$ μm as the variation in radius alone has been used here to account for the maximum possible shift in the position of the MDR. The fitting of the experimental spectra with the simulations shows that up to three orders of the MDR are observed here.

It is seen that the first-order and second-order modes

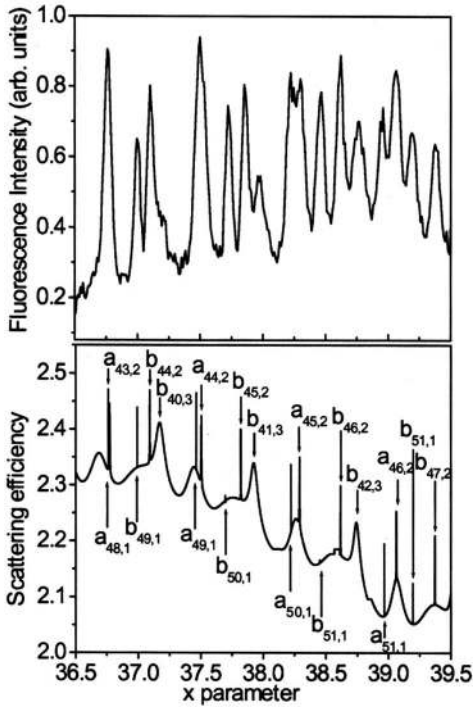

FIG. 3. A part of the observed fluorescence spectrum [curve (D) in Fig. 2] fitted with the scattering efficiency simulation for a single PMMA microsphere (refractive index=1.49) with a radius of 2.807 μm.

TABLE I. Quality factors of the observed MDR (Q_{obs}) for various modes (for brevity of presentation, half of the observed modes are not listed here) of first, second, and third orders as a function of the concentration of doping.

	$Q_{obs}(\pm 0.2\times 10^2)$		
	Concentration of 9AAHH		
Mode[a]	0.5 mM($\times 10^2$)	20 mM($\times 10^2$)	100 mM($\times 10^2$)
$b_{44,1};b_{39,2}$	4.41	4.15	4.15
$a_{39,2}$	7.24	6.98	6.98
$b_{45,1};b_{40,2}$	5.29	5.29	5.29
$a_{40,2}$	5.35	5.35	4.28
$a_{45,1}$	5.36	[b]	5.37
$b_{46,1};b_{41,2}$	4.32	4.33	4.33
$b_{48,1}$	[b]	[b]	5.63
$b_{43,2}$	5.65	5.65	5.65
$b_{49,1}$	5.75	5.76	5.75
$b_{44,2}$	5.77	5.77	5.77
$a_{49,1};a_{44,2}$	3.89	3.89	3.88
$b_{50,1}$	5.87	5.87	5.86
$b_{45,2}$	5.89	5.89	5.89
$b_{41,3}$	3.94	3.93	3.94
$a_{50,1}$	5.95	5.95	5.94
$b_{42,3}$	4.03	4.02	4.02
$b_{52,1}$	6.10	[b]	6.10
$b_{47,2}$	6.14	6.13	6.12
$b_{43,3}$	4.93	4.92	4.70
$a_{52,1}$	6.12	6.17	6.17
$b_{48,2}$	6.25	6.25	6.24
$a_{53,1};b_{44,3}$	4.19	4.18	2.79
$b_{54,1};a_{48,2}$	4.22	4.22	3.62
$b_{49,2}$	6.37	[b]	6.36
$a_{54,1};b_{45,3}$	5.12	5.12	3.65
$b_{55,1};a_{49,2}$	4.29	3.22	3.22

[a]Mode numbers $b_{44,1}-b_{44,3}$ fall in the region free from the overlap of absorption, while $a_{53,1}-b_{55,1}$ fall in the spectral overlap region.
[b]Too weak to be calculated.

appear strongly in the experimental spectra while the modes of the higher orders are weaker. The quality factors (Q_{obs}) for the various observed modes are given in Table I. The Q_{obs} values of the individual modes are evaluated as $Q_{obs}=x/\gamma$ where x is the x parameter of the peak value and γ is the FWHM of the individual mode. Figure 2 also shows that the MDR of the different orders coexists at nearly equal x parameters at various regions of the spectra with a varying degree of overlap among them. For a partial overlap of two MDRs, after fitting with a Lorentzian line shape, the half value of the observed FWHM of the individual peak was used for obtaining the Q_{obs} values. The experimentally observed values in this manner are sufficiently accurate to discuss the following.

Increasing the concentration of the doping solution does not show any appreciable change in the Q_{obs} values of the individual MDR in the regions free from the spectral overlap (x-parameter range of 33–41). For example, the MDR $b_{46,1}$ has a Q_{obs} value of 4.33×10^2 irrespective of the concentration of the molecules. In the x-parameter range of 41–42, there is an overlap of the fluorescence with the absorption of the molecule. The mode $a_{54,1}$ which falls in this region (and experiences maximum absorption effect) measures a Q_{obs} value of 5.12×10^2 for the curves (A)–(C) but drops down to 3.65×10^2 for the highest concentration. This indicates that till curve (C) an increase in the concentration of the doping does not introduce any change in the imaginary part of the refractive index of the microsphere but for curve (D) it decreases the value of Q_{obs} slightly due to the appearance of an additional quality factor due to absorption (Q_a). In such case the Q_{obs} is given by[27]

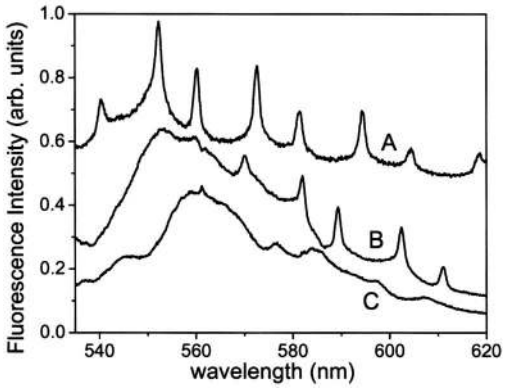

FIG. 4. Fluorescence spectra of Rhodamine 6G in ~2-μm-radius single PMMA microsphere as a function of concentration. The concentrations are (A) 5 mM, (B) 10 mM, and (C) 100 mM.

$$\frac{1}{Q_{obs}}=\frac{1}{Q_0}+\frac{1}{Q_a}, \tag{6}$$

where Q_0 represents the quality factor calculated for the real value of the refractive index of the microcavity.

It can be seen further from Fig. 2 that the relative intensities of the MDR peaks are reduced for higher concentrations of the dye towards higher x parameters. For curve (D) the MDR peaks are very weak in the overlap region. We have observed also that for a case of strong overlap between the absorption and fluorescence emission such as that in Rhodamine 6G, MDR disappears completely at higher concentrations (Fig. 4). Hence for further experiments we chose the doping concentrations [in the range of curves (A) and (B) in Fig. 2] such that the spectral region is free from the self-absorption effect. This gives an opportunity to study the effect of the variation in the adsorbed concentration without any effect on Q_{obs}. Table I also indicates that the effect of self-absorption on the Q_{obs} values of the second- and third-order modes is negligible. This is due to the fact that the concentration of the molecules in these doped microspheres is highest at the surface as compared with the inner regions where the higher-order modes exist.[28]

B. Effect of MDR on radiative rate

To calculate the radiative rate, the fluorescence lifetime of 9AAHH embedded in single PMMA microspheres was measured. A single exponential fluorescence decay intensity (I) is given as

$$I=A_0e^{-t/\tau_0}, \tag{7}$$

where A_0 is the preexponential factor and τ_0 is the fluorescence lifetime of the molecule. In the presence of another

TABLE II. The fluorescence lifetimes and amplitudes for 9AAHH for single microspheres of PMMA doped with 0.5 mM 9AAHH (λ_{exc}=408 nm).

Diameter (μm)	$\tau_1 \pm 0.01$ (ns)	$\tau_2 \pm 0.01$ (ns)	B_1	B_2	χ^2
20	⋯	12.16	⋯	1.00	1.04
18	⋯	12.05	⋯	1.00	1.08
15	⋯	12.31	⋯	1.00	1.09
12	⋯	12.28	⋯	1.00	0.99
10	7.56	12.99	0.20	0.80	1.03
9	4.29	12.30	0.19	0.81	0.99
7	2.07	12.30	0.22	0.78	1.01
6	1.05	12.24	0.39	0.61	0.99
5	0.90	11.93	0.76	0.24	1.15
4	0.83	11.76	0.85	0.15	0.99
3	0.78	10.41	0.84	0.16	1.02

competing decay rate in the excited state, the behavior is given by the biexponential decay scheme,

$$I = B_1 e^{-t/\tau_1} + B_2 e^{-t/\tau_2}, \tag{8}$$

where B_1 and B_2 are the amplitudes of the lifetime components τ_1 and τ_2, respectively.

Table II gives the fluorescence lifetime data for microspheres doped with a concentration of 0.5 mM of 9AAHH. For a 20-μm-diam. microsphere, the observed decay curve fits to the single exponential decay function with a time constant of 12.16 ns. This value of the fluorescence lifetime of 9AAHH is close to that observed in the thin films of another polymer polyvinyl alcohol (12.27 ns). A reduction of the diameter of the single microsphere down to 12 μm does not show any change in the fluorescence decay. However, a further reduction in the diameter of the microsphere to 10 μm results in the appearance of an additional (faster) component in the fluorescence decay profile. The new component with a decay time of 7.56 ns has a smaller amplitude (20%) relative to the former. A further decrease in the microsphere diameter is followed by a decrease of the decay time of the new component with concomitant increase in its amplitude. For a microsphere of ~3 μm diameter, the new component has a decay time of 780 ps with an amplitude of 84%, whereas the slow component shows a decay time of 10.40 ns with an amplitude of 16%. Figure 5 (panel A) shows the fitted curve of a biexponential behavior of the fluorescence decay from a ~3-μm-diam. single microsphere. It can be seen clearly (from panels B and C) that the fluorescence data fit well with a biexponential decay function. Panel D shows the behavior of the amplitudes of the slower and faster components below the threshold value (10 μm). While the faster component shows an increase in the amplitude, the slower component decreases in its amplitude on the reduction of the diameter of the microsphere.

Given the fact that the other nonradiative processes do not exhibit the size effect at room temperature (300 K), we attribute this shortening of fluorescence lifetime to the RRE of the molecule as mentioned in Sec. III B. The RRE (ξ) which is a measure of the increase in the radiative rate of the molecule shows a >15-fold increase for a ~3-μm-diam. particle as compared with the bulk. This behavior is shown in Table III as a function of the concentration.

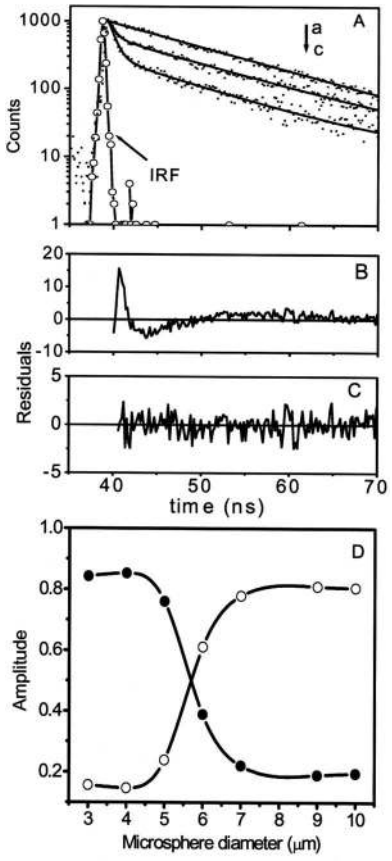

FIG. 5. Panel A gives the decay data of 9AAHH in PMMA single microspheres with diameters as (a) 20 μm, (b) 5 μm, and (c) 3 μm along with the corresponding fits shown in Table I (—). IRF represents the instrument response function. Panel B gives the residual for a single exponential fit while the residual for a biexponential fit is given in panel C for the data of curve (c). Panel D gives the amplitudes for the fast (-●-) and slow (-○-) components of the biexponential fluorescence decay from single microspheres.

For a higher adsorbed concentration, although the decay data exhibit a similar pattern, the magnitude of RRE is found to decrease. For instance, for a concentration of 3.5 mM, the value of ξ for a 3-μm-diam. microsphere reduces to 5.94 as compared with 15.76 observed for the 0.5 mM. This indicates that the RRE decreases by ~10 for a sevenfold increase in the concentration of the molecules. A plot of the RRE as a function of the microsphere diameter is given in Fig. 6 for the three concentrations studied here.

TABLE III. The RRE of the faster component of 9AAHH in single microspheres of varying concentrations as a function of the microsphere diameter.

Diameter (μm)	RRE (ξ)[a]		
	0.5 mM	1 mM	3.5 mM
3	15.76	8.43	5.94
5	12.78	6.39	4.52
6	11.64	5.72	3.78
8	6.03	2.75	2.55
10	1.62	1.58	1.48

[a]The value of RRE is taken as 1.0 for the bulk.

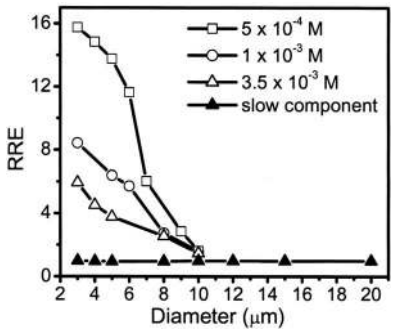

FIG. 6. The RRE (ξ) plotted as a function of the diameter of the single PMMA microsphere for varying doping concentrations.

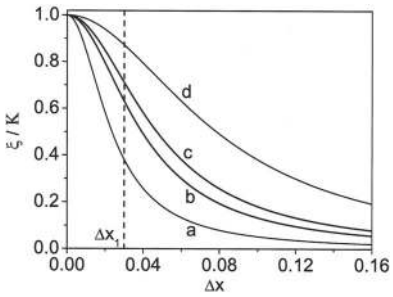

FIG. 7. The variation of the change in enhancement of the radiative rate with the detuning of the x parameter for microsphere diameters of (a) 3 μm, (b) 5 μm, (c) 6 μm, and (d) 10 μm.

C. RRE and the introduction of detuning parameter

It is known theoretically[10–12] that the RRE can be influenced due to (i) the change in the Q of the interacting MDR (Ref. 27) and (ii) a shift in the peak frequency of the MDR from that of the homogeneous linewidth.[12] This shift is termed here as the detuning parameter (δ). As seen from Table I no reduction in Q is observed in the concentration range studied here. Hence we consider case (ii). The shift in the MDR frequency can occur by a change in the refractive index of the microsphere as well as in its radius. However, by considering the fact that the spectra shown for the microspheres in Fig. 2 are consistent within the particle diameter of 2.805 ± 0.004 μm, we propose that the effective changes in the real part of the refractive index are responsible for the observed reduction of ξ with the doping concentration (Table III). This change in the refractive index is caused due to a difference in the adsorbed concentration on the microspheres doped with various concentrations. This is consistent with the reported increase in the refractive index of a microcylinder with an increase in the doping concentration.[29] This is understood as an increase in the dispersing ability of the medium by an increase in the molecular density. Typical calculations of Q_{sca} indicate that a change in the refractive index of ~ 0.001 causes a shift in the x parameter (Δx) of the mode $b_{50,1}$ by ~ 0.0246.

The Q values of the MDR observed experimentally are found to be of the order of 10^2 (Table I). This is a case of weak coupling in which the enhancement agrees with an evaluation based on Fermi's golden rule. Under this condition an explicit relation for the enhancement of the radiative rate for a two-level system, incorporating the detuning parameter (δ), is given as[12]

$$\xi = K \frac{(\gamma/2)^2}{\delta^2 + (\gamma/2)^2}. \tag{9}$$

Here K represents the maximum possible RRE (ξ) when the MDR frequency coincides with the fluorescence peak ($\delta = 0$). However, to the best of our knowledge, any experimental work verifying this equation in the case of dye-doped single microspheres does not exist in literature.

D. Comparison with the simulations of detuning parameter

As shown in Fig. 1, the RRE depends upon the fact of whether a MDR falls exactly on the homogeneous linewidth of the fluorescing molecule. In order to investigate the effect of the shift (detuning) of the MDR from the homogeneous linewidth, simulations were carried out for the ratio of the observed RRE to that of the maximum possible RRE (ξ/K) as a function of the detuning parameter for various values of the microsphere diameter by using Eq. (9). The detuning parameter can be expressed in terms of the x parameter as $\Delta x = 2\pi r \delta$. The calculations were made for a fixed value of the FWHM of the MDR (γ) of 50 cm^{-1} which is close to the experimentally observed value for the first-order modes in this work. In addition it is $\sim$ four times smaller compared with the reported value of the homogeneous linewidth of 9AAHH in PMMA at 300 K (Ref. 21) fulfilling the condition of $\Gamma_h > \gamma$ required by Eq. (5).

The observed enhancement normalized to K has been plotted as a function of the change in x parameter (Δx) for various microsphere diameters in Fig. 7. It can be seen that with an increase in detuning, the ratio falls rapidly following a Lorentzian function. A small change in the x parameter affects the observed enhancement. While for a 3-μm-diam. microsphere the RRE ratio falls by half for a change in the value of $x \sim 0.025$; for a 10 μm microsphere it needs a corresponding change of 0.08. In other words, for a constant value of the detuning parameter, the decrease in the RRE ratio is smaller for larger diameter microspheres. For a detuning parameter value of 0.03 (indicated as Δx_1 in Fig. 7) the RRE ratio decreases by 2.5 times of its initial value for a microsphere of 3 μm diameter, whereas it decreases by only 1.1 times of its initial value for a 10-μm-diam. microsphere. This result is in agreement with our experimental observations. As seen from Table III with a sevenfold increase of the concentration, the RRE is distinctly reduced by a factor of ~ 2.65 of its initial value in the case of the 3-μm-diam. microsphere in comparison with a reduction of ~ 1.1 of its initial value in the case of the 10-μm-diam. microsphere.

The magnitude of the RRE decreases (Fig. 6) and hence, the MDR detuning (based on the aforementioned discussion) increases with an increase in the adsorbed concentration of the dye molecule. From the Clausius-Mossotti relationship,[30] the changes in the refractive index per mass of the material are additive in nature. The change in the refractive index is

thus proportional to the change in the number of the adsorbed molecules. It is also observed that the detuning increases with a decrease in the diameter of the microsphere. These observations are also consistent with the theoretical understanding proposed by Arnold *et al.*[23] showing a direct proportionality of the shift of the MDR with the surface density of the adsorbed molecule on the microsphere and an inverse proportionality to the radius of the single microsphere.

For large detuning in two-level atomic systems, the RRE values of the order of 10^3-10^4 have been calculated by Chew[10,11] and Lai *et al.*[12] However, the experimentally observed RRE values in molecules embedded in dielectric microspheres (including this work) are of the order of 10.[17–21] Nevertheless, it is observed that the theoretical simulations presented here provide relevant information towards the behavior of molecular systems in a single microsphere.

V. CONCLUSIONS

In conclusion, the modification in the radiative rate of molecules confined in a single spherical microcavity as a function of the adsorbed molecular density is reported here. For nearly transparent microspheres, while the Q value of the MDR is found to remain the same, the RRE has been found to decrease with the increase in the molecular density in the single microsphere. This has been attributed to the increased dispersion in the microsphere (change in the refractive index) on increasing the dye concentration. The resultant shift in the MDR from the homogeneous linewidth of the molecule has been found to be responsible for the change in RRE. It is found that for the smallest microcavity studied here, the RRE reduces by ~ 10 for a sevenfold increase in the adsorbed dye concentration.

ACKNOWLEDGMENTS

We thank DST, New Delhi and DRDO, New Delhi for the financial assistance during the course of this work.

[1] R. E. Benner, P. W. Barber, J. F. Owen, and R. K. Chang, Phys. Rev. Lett. **44**, 475 (1980).
[2] P. W. Barber and S. C. Hill, *Light Scattering by Particles: Computational Methods* (World Scientific, Singapore, 1990).
[3] R. K. Chang and A. J. Campillo, *Optical Processes in Microcavities* (World Scientific, Singapore, 1996).
[4] P. B. Bisht, K. Fukuda, and S. Hirayama, J. Chem. Phys. **105**, 9349 (1996).
[5] S. X. Qian, J. B. Snow, H. M. Tzeng, and R. K. Chang, Science **231**, 486 (1986).
[6] S. M. Spillane, T. J. Kippenberg, and K. J. Vahala, Nature (London) **415**, 621 (2002).
[7] S. D. Druger, S. Arnold, and L. M. Folan, J. Chem. Phys. **87**, 2649 (1987).
[8] G. S. Agarwal and S. D. Gupta, Phys. Rev. A **57**, 667 (1998).
[9] F. Volmer, D. Braun, A. Libchaber, M. Khoshsima, I. Teraoka, and S. Arnold, Appl. Phys. Lett. **80**, 4057 (2002).
[10] H. Chew, J. Chem. Phys. **87**, 1355 (1987).
[11] H. Chew, Phys. Rev. A **38**, 3410 (1988).
[12] H. M. Lai, P. T. Leung, and K. Young, Phys. Rev. A **37**, 1597 (1988).
[13] H. Yokoyama and S. D. Brorson, J. Appl. Phys. **66**, 4801 (1989).
[14] S. Arnold, J. Chem. Phys. **106**, 8280 (1997).
[15] F. L. Kien, N. H. Quang, and K. Hakuta, Opt. Commun. **178**, 151 (2000).
[16] H. T. Dung, L. Knoll, and D. G. Welsch, Phys. Rev. A **62**, 053804 (2000).
[17] H. B. Lin, J. D. Eversole, C. C. Merritt, and A. J. Campillo, Phys. Rev. A **45**, 6756 (1992).
[18] M. D. Barnes, W. B. Whitten, and J. M. Ramsey, Chem. Phys. Lett. **227**, 628 (1994).
[19] M. D. Barnes, W. B. Whitten, and J. M. Ramsey, J. Opt. Soc. Am. B **11**, 1297 (1994).
[20] H. Fujiwara, K. Sasaki, and H. Masuhara, J. Appl. Phys. **85**, 2052 (1999).
[21] P. Sandeep and P. B. Bisht, Chem. Phys. Lett. **371**, 327 (2003).
[22] E. Krioukov, J. Greve, and C. Otto, Sens. Actuators B **90**, 58 (2003).
[23] S. Arnold, M. Koshsima, I. Teraoka, S. Holler, and F. Vollmer, Opt. Lett. **28**, 272 (2003).
[24] I. Teraoka, S. Arnold, and F. Vollmer, J. Opt. Soc. Am. B **20**, 1937 (2003).
[25] M. Noto, F. Vollmer, D. Keng, I. Teraoka, and S. Arnold, Opt. Lett. **30**, 510 (2005).
[26] E. M. Purcell, Phys. Rev. **69**, 681 (1946).
[27] P. Chylek, H. B. Lin, J. D. Eversole, and A. J. Campillo, Opt. Lett. **16**, 1723 (1991).
[28] G. Mie, Ann. Phys. **25**, 377 (1908).
[29] M. Ohashi and M. Tateda, J. Lightwave Technol. **11**, 1941 (1993).
[30] C. Kittel, *Introduction to Solid State Physics*, 7th ed. (Wiley, Singapore, 1995), p. 390.